energies

MDPI

Article

# Analyzing the Impact of Renewable Energy Incentives and Parameter Uncertainties on Financial Feasibility of a Campus Microgrid

**Vu Ba Hau [1], Munir Husein [1], Il-Yop Chung [1,*], Dong-Jun Won [2], William Torre [3] and Truong Nguyen [3]**

1 School of Electrical Engineering, Kookmin University, 861-1, Jeongneung-dong, Seongbuk-gu, Seoul 02707, Korea; vubahau@kookmin.ac.kr (V.B.H.); munir@kookmin.ac.kr (M.H.)
2 Department of Electrical Engineering, Inha University, 100, Inha-ro, Michuhol-gu, Incheon 402-751, Korea; djwon@inha.ac.kr
3 University of California San Diego, 9500 Gilman Drive, La Jolla, CA 92093, USA; wtorre@ucsd.edu (W.T.); tqn001@eng.ucsd.edu (T.N.)
* Correspondence: chung@kookmin.ac.kr; Tel.: +82-2-910-4702; Fax: +82-2-910-4449

Received: 17 August 2018; Accepted: 12 September 2018; Published: 14 September 2018

**Abstract:** The popularity of microgrids is increasing considerably because of their environmental and technical advantages. However, the major challenge in microgrid integration is its financial feasibility due to high capital costs. To address this obstacle, renewable energy incentive programs, which are the motivation of this study, have been proposed in many countries. This paper provides a comprehensive evaluation of the technical and financial feasibility of a campus microgrid based on a techno-economic analysis using the Microgrid Decision Support Tool, which was implemented to support decision-making in the context of microgrid project investment. A method for microgrid design aiming to maximize system profitability is presented. The optimal microgrid configuration is selected depending on financial indices of the project, which directly address the returns on an investment. Most importantly, this analysis captures all the benefits of financial incentives for microgrid projects in California, U.S., which presents a key difference between the California market and other markets. The impact of incentives and uncertain financial parameters on the project investment is verified by sensitivity analysis. The outcomes show that the optimal configuration generates significant electricity savings, and the incentives strongly determine the financial feasibility and the optimal design of a microgrid.

**Keywords:** microgrid design; financial feasibility analysis; renewable energy incentives; tax credits

## 1. Introduction

In recent years, electric power system design has witnessed a paradigm shift from the traditional centralized grid system toward decentralized and independent systems called microgrids, which can operate in either the grid-connected or islanded mode to supply demand targets. Researchers have increasingly been focusing on microgrids because they offer obvious advantages, such as high penetration of renewable energy resources (RESs), improved reliability due to the autonomous operation of distributed energy resources (DERs), and significant reductions in greenhouse gas emissions as well as reductions in a power system's operating costs. Specifically, the optimal design of a microgrid considering economic and dynamic performance analysis was presented in reference [1], which contains photovoltaics (PV), wind turbines, a battery energy storage system (BESS), and two diesel generators. The study indicated important benefits by microgrid adoption such as minimization of levelized cost of energy (LCOE), maximization of renewable energy penetration and significant

reductions in fuel consumption. The technical benefits of energy storage system (ESS) utilization in a microgrid was determined in reference [2], which included reducing peak load, providing standby power, and enhancing power quality. Similarly, the advantages of a microgrid comprising PV and ESS was indicated in reference [3]. Regarding the ability of a microgrid to reduce emissions, an optimal microgrid design considering net zero emissions as an environmental constraint was presented in reference [4]. The study in reference [5] also highlighted significant reductions in carbon dioxide emissions by a microgrid, including biomass energy for rural electrification. The dynamic operation, transient stability, power efficiency and control of microgrid systems has been well developed and evaluated in the literature. The research presented in reference [6] examined the dynamic operation and control strategies for a microgrid hybrid power system, and an intelligent controller for maximum power point tracking (MPPT) control was proposed, which enables the hybrid generation system to effectively extract the maximum power. The optimal operation of microgrids using multi-agent system was presented in reference [7], which considered changes in the microgrid configuration due to the addition or removal of an energy unit. In reference [8], the transient stability in a hybrid power system was improved using a novel intelligent damping controller, which was designed for the static synchronous compensator to reduce the power fluctuation, voltage support, and damping in the system operation. In addition, the fault analysis and protection methods for microgrid distribution systems were proposed considering various types of fault [9,10]. In summary, it is clear that the technical impact and operational feasibility of microgrid systems have been convincingly validated.

In the design stage of a microgrid system, it is fundamental to perform a techno-economic analysis, which helps determine whether a particular microgrid configuration is technically and financially feasible [11]. From an economic perspective, one of the challenges in the integration of renewable energy technologies is their higher investment capital compared to conventional technologies [12,13]. To overcome this problem, technological innovation plays an important role in substantially reducing the installation costs of DERs and energy storage technologies [14,15]. In addition, many countries have launched financial incentive programs to promote the adoption of renewable energy systems. Numerous previous studies have evaluated the economics of microgrids considering real market conditions and policies, and the most recent studies are reported in this section. In reference [16], the economics of local energy provision was examined considering market conditions in Southern California to determine the optimal configuration for different microgrid business models. The optimal selection and sizing of DERs were based on the cost savings and economic benefits of self-supply by microgrid adoption. However, demand-side flexibilities and renewable energy incentives, which directly impact energy savings and enhance the benefits of microgrid design, were not included in the analysis. In reference [17], an optimization model based on mixed integer linear programing (MILP) for BESS operation in conjunction with PV modules was proposed to determine the optimal configuration with the objective function of maximizing revenue streams under feed-in tariff, which was the only incentive included in the study. The analysis presented in reference [18] investigated the economic benefits of the optimal location of DERs in a microgrid, and the cost reduction was addressed in the absence of any capital grants. The economic analyses of microgrids in references [16–18] were performed using the Distributed Energy Resources Customer Adoption Model (DER-CAM) modeling framework, which uses before-tax cash flow calculations. In references [19,20], photovoltaic-battery storage systems were studied with their own proposed energy dispatch schedule optimization, and system economics were quantified based on net present value (NPV) of the battery without addressing the benefits of incentives for PV and batteries, which directly improve cash inflows. In reference [21], an economic analysis for planning purposes was conducted considering incentives and taxes, but this analysis did not solve the optimal sizing problem for DERs. In summary, these studies have the following limitations: They did not investigate the financial feasibility of microgrids; they did not include incentives in their economic analysis, which would substantially enhance system profitability; and/or they conducted analyses using before-tax calculations, which ignore the benefits arising from renewable energy tax credits and tax deductions. The research

presented in reference [22] highlighted that the impact of tax benefits can vary considerably from one microgrid configuration to another. Therefore, comparing alternatives on an after-tax basis is imperative for valid economic analysis.

In this study, a method for determining the optimal design of microgrids based on financial feasibility analysis is presented with the aim of maximizing project profitability. In addition to the economic benefits derived by local energy provision, this method incorporates all revenues from renewable energy incentives, tax credits, and tax deductions by performing analysis on after-tax cash flows. The technique was applied to obtain the optimal design for a campus microgrid in California, U.S. The primary reason why California was selected as a case study is because of its diversity of incentive programs for renewable energy and energy efficiency projects [23]. The technologies considered for the campus microgrid include PV, ESS, and fuel cell (FC) because they are eligible for various incentive programs offered by the state and federal government. The incentives evaluated in this study are energy investment tax credit (ITC), investment-based incentive (IBI), net metering, depreciation and property tax incentive. In addition, the analysis considered the potential economic benefits of implementing load control with demand side management (DSM) in the microgrid, which contributes to energy savings. Finally, a sensitivity analysis of parameter uncertainties and incentive rates was conducted to evaluate their impact on the optimal configuration and financial feasibility of the microgrid. It was found that the optimal microgrid configuration resulted in reductions in electricity costs by 49.21%, and the project profitability was greatly enhanced when after-tax cash flow was used to quantify the tax benefits for renewable energy technologies. The results also indicated that financial incentives significantly affect the optimal microgrid design including both the optimal mix and sizing of DER units. Therefore, incorporating grant incentives and tax benefits in the economic evaluation of microgrids is crucial to have an effective design.

All of the simulations in the present study were conducted using MDSTool developed by us for the techno-economic analysis of hybrid renewable energy systems [22]. MDSTool was created with the purpose of evaluating microgrid business models, which can address all of the economic benefits of a microgrid project. The tool is based on an open architecture implemented in the MATLAB programing environment, which offers several advantages compared to other commercial tools such as HOMER, iHOGA, HYBRID2 and SAM [22]. Due to its open architecture, users can define and develop new dispatch algorithms, while assumptions and constraints can be modified and added, and technology models can be changed. In addition, a detailed financial structure specific to a region or country can be incorporated. The most important feature of MDSTool is that it provides both pre-tax and after-tax cash flow analysis, and is designed to incorporate any types of incentive and credit for different renewable energy technologies in a microgrid project.

The remainder of this paper is organized as follows. Section 2 describes the structure of MDSTool and the microgrid design methodology arising from its application. Section 3 summarizes the data of a case study performed in this paper. Section 4 presents the results, discussion, and further analyses for the case study. Finally, our conclusions are provided in Section 5.

## 2. Microgrid Design with MDSTool

MDSTool was developed to solve design and planning problems associated with hybrid renewable energy systems. The tool is used to determine the optimal configuration of a microgrid, which considers the optimal DER mix, DER capacity, and DER dispatch strategy, based on techno-economic analysis, which calculates all of the costs incurred by, and benefits derived from, a project over its lifetime. The structure of MDSTool is described in Figure 1. It comprises two computation models, which are a performance model and an economic model. The performance model simulates the system operation optimization for one year, and records all of the energy generation and consumption profiles, which are then used as inputs for the economic model. Subsequently, the economic model computes all cash flows over the lifetime of the project to determine economic measures required for optimal DER sizing and financial feasibility analysis. A detailed description of MDSTool can be found in reference [22].

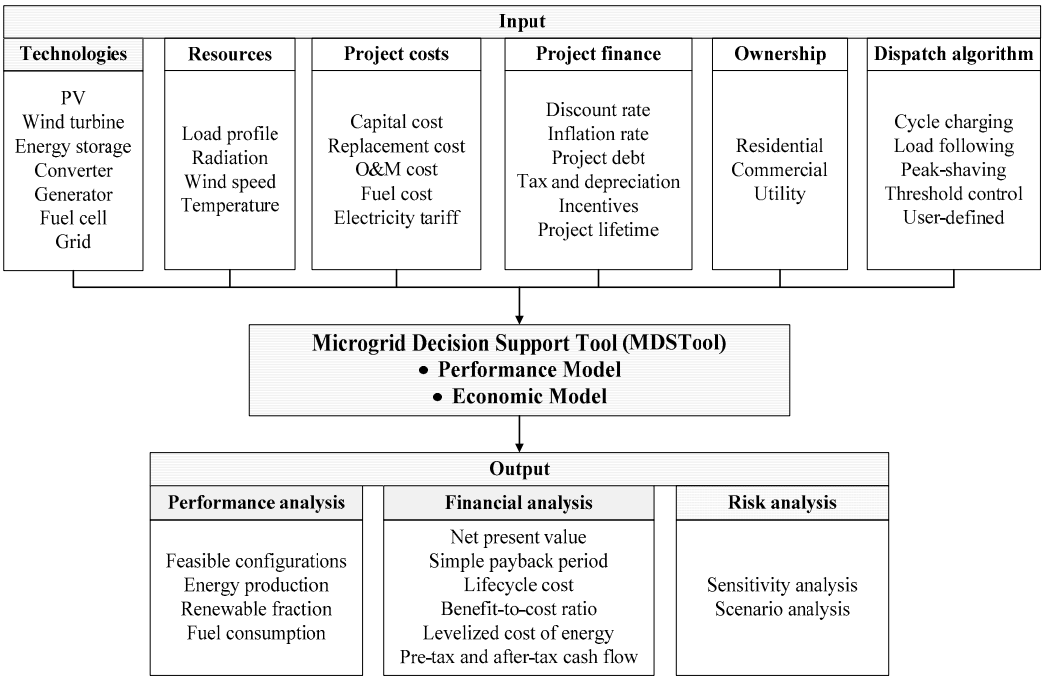


**Figure 1.** The structure of MDSTool.

## 2.1. Performance Model

The performance model simulates one-year power generation and consumption for each microgrid configuration in a search space which contains all of the possible capacities and combinations of DERs defined by the user. The inputs for the performance model include 8760-h time-series data of electricity load demands and weather resources, such as solar irradiance and wind speed, the technical specifications and cost parameters of DERs and a user-defined economic dispatch algorithm. The output is a set of time-series data which details hourly energy production and consumption within the system. The mathematical modeling of DERs is the primary determinant of the accuracy of this model. MDSTool employs time-series behavioral models used for long-term performance prediction and evaluation. Currently, the technologies modeled in MDSTool consist of PV, wind turbines, geothermal energy, biomass, internal combustion engines, FCs and energy storage. As the microgrid used as a case study in this paper contains a PV, a BESS, and an FC, their mathematical models are presented here.

### 2.1.1. PV Model

PV modules are rated on the basis of the power generated under the standard testing condition (STC) of 1 kW/m$^2$ of sunlight and a PV cell temperature of 25 °C. Various performance models for PV modules were developed [24,25]. The power produced by PV modules can be calculated as a function of solar irradiance, as given in Equation (1).

$$P_{pv}(t) = P_{pv,STC} \cdot \frac{G_T(t)}{G}[1 + K_T(T_{cell}(t) - T_{STC})] \quad (1)$$

### 2.1.2. BESS Model

MDSTool uses the battery model developed by Manwell and McGowan [26], which is based on the concept of electrochemical kinetics, and can determine the charge and discharge power from a

battery at each time step. The maximum amount of power that a battery can discharge and charge over time step Δt [h] is given by Equations (2) and (3), respectively.

$$P_{\max d} = \frac{-kcQ_{\max} + kQ_1 e^{-k\Delta t} + Qkc(1 - e^{-k\Delta t})}{1 - e^{-k\Delta t} + c(k\Delta t - 1 + e^{-k\Delta t})} \tag{2}$$

$$P_{\max c} = \frac{-kQ_1 e^{-k\Delta t} + Qkc(1 - e^{-k\Delta t})}{1 - e^{-k\Delta t} + c(k\Delta t - 1 + e^{-k\Delta t})} \tag{3}$$

A power electronic converter is modeled as a black box and the modeling is undertaken using an efficiency, which reflects the power loss between the input and output.

#### 2.1.3. FC Model

FC is considered to be generator with generation cost model using fuel cost curve, in which the fuel consumption as a function of the electrical output power is assumed to be linear as in reference [27]:

$$f(t) = x \cdot P_r + y \cdot P_{gen}(t) \tag{4}$$

#### 2.1.4. DER Dispatch Model

To perform the system operation optimization, a dispatch algorithm for DERs must be specified. This dispatch algorithm involves the problem of unit commitment and economic dispatch of DERs. At each time step, the algorithm decides which components will operate and at what power level to efficiently supply the load demand at a minimum operating cost while satisfying operational constraints. The objective function is described by Equation (5) followed by its constraints.

$$\min C_{total,t} = C_{gen,t} + C_{dch,t} + C_{gbuy,t} - C_{gsell,t} - C_{dres,t} - C_{anc,t} \tag{5}$$

subject to the following constraints:

$$P_{load,t} = P_{G,t} + P_{S,t} + P_{gbuy,t} - P_{gsell,t} \tag{6}$$

$$\begin{aligned} &P_g^{\min} \le P_{g,t} \le P_g^{\max} \\ &P_{dch,t} \le P_{dch,t}^{\max} \\ &P_{gbuy,t} \le P_{gbuy,t}^{\max} \\ &P_{gsell,t} \le P_{gsell,t}^{\max} \end{aligned} \tag{7}$$

$$SoC_{\min} \le SoC_t \le SoC_{\max} \tag{8}$$

Equation (6) describes the energy balance constraint between energy demand and supply at each time step. The set of Equation (7) shows the inequality constraints controlling the output power of the energy sources, as well as the purchase from and sale to the grid to satisfy the maximum and minimum thresholds. Equation (8) indicates that the SoC of storage units must be maintained between the maximum and minimum values.

The optimization of system operation is performed at each time step, and this is repeated 8760 times to complete the one-year operation of a configuration. Subsequently, the performance model decides whether a configuration is technically feasible based on reliability constraints. MDSTool utilizes the two most widely used reliability metrics: Loss-of-load probability (LOLP) and loss-of-power supply probability (LPSP) [28]. As a result, the energy generation and consumption profiles of feasible configurations are saved and used as the inputs for the economic model, which calculates all cash flows for financial feasibility and optimal sizing analyses.

### 2.2. Economic Model

MDSTool uses cash flow analysis, which accounts for all expenses (cash outflows) and benefits (cash inflows). The pre-tax cash flow calculates the total installation and operating costs, and all project revenues, while the after-tax cash flow includes all debt payments and income tax considering tax benefits from debt interest payments, depreciation and tax credits such as ITC and production tax credit (PTC) [22].

The pre-tax cash outflows and inflows are calculated using Equations (9) and (10), respectively. The only pre-tax cash outflow in year zero is the project equity, while the cash outflows in subsequent years account for all costs incurred over the project's lifetime. The pre-tax cash inflow in year zero is equal to any IBI. In subsequent years, the pre-tax cash inflows are all project revenues.

$$F_{out,n} = \begin{cases} C_{install}(1-f_d) & (n=0) \\ C_{annual}(1+r)^n + C_{prt}\left[1-\phi_{pvd}(n-1)\right] + C_{emsp} & (n>0, n \neq N_R) \\ (C_{annual}+C_{rep})(1+r)^n + C_{prt}\left[1-\phi_{pvd}(n-1)\right] + C_{emsp} & (n=N_R) \end{cases} \quad (9)$$

where $C_{annual} = C_{o\&m} + C_{gbuy} + C_{fuel} + C_{ins}$

$$F_{in,n} = \begin{cases} C_{ibi} & (n=0) \\ C_{pbi} + C_{grev}(1+r)^n + C_{emsc} & (n=1,2,\ldots,N-1) \\ C_{pbi} + (C_{grev}+C_{salv})(1+r)^n + C_{emsc} & (n=N) \end{cases} \quad (10)$$

The total pre-tax cost in each year is the net difference between pre-tax cash inflows and cash outflows. The total pre-tax cash flow is calculated by adding the benefits from energy savings to the pre-tax cost.

$$F_{PTC,n} = F_{in,n} - F_{out,n} \quad (11)$$

$$F_{PTCF,n} = F_{PTC,n} + C_{saving}.(1+r)^n \quad (12)$$

In the after-tax basis, the total after-tax cost is determined by subtracting the total debt payment and income tax from $F_{PTC}$, while the total after-tax cash flow is determined by adding after-tax savings to $F_{ATC}$. To capture tax benefits for tax-paying investors, the calculation of income tax accounts for tax deductions from debt interest payments, depreciation, and tax credits for DERs [22].

$$F_{ATC,n} = F_{PTC,n} - C_{debt,n} - C_{tax,n} \quad (13)$$

$$F_{ATCF,n} = F_{ATC,n} + \delta \cdot C_{saving} \cdot (1+r)^n \quad (14)$$

$$\delta = \delta_s + \delta_f.(1-\delta_s) \quad (15)$$

The total costs and cash flows can be used to calculate different financial indices used for optimal selection of DERs and financial feasibility analysis. MDSTool provides standard financial metrics such as NPV, lifecycle cost (LCC), benefit-cost ratio (BCR), simple payback period (SPB), internal rate of return (IRR), and annual lifecycle savings (ALCS). Hereby, MDSTool provides both pre-tax and after-tax cash flow analysis. The choice of pre-tax or after-tax analysis depends on the ownership of a microgrid project. Pre-tax financial analysis is appropriate for non-tax-paying investors such as governmental agencies, while after-tax analysis is crucial for private entities investing in microgrids because taxes and tax credits are real costs which directly affect cost and revenue streams of a commercial investment.

### 2.3. Microgrid Design Using MDSTool

The purpose of this study is to provide an optimal microgrid design methodology for commercial ownership based on financial feasibility analysis, which can capture all of the benefits from renewable

energy incentives and tax reduction programs and evaluates their impact on the investment. For this reason, this method uses after-tax basis to compare alternative configurations.

With the objective of addressing all benefits and returns by a microgrid deployment, the metrics used in this study for financial feasibility evaluation are NPV, SPB, LCC, and BCR. NPV is computed by subtracting the present values of cash outflows from the present values of cash inflows over the lifetime of the investment, as shown in Equation (16). It is a direct measurement that determines to what extent an investment will be profitable. In the context of investment decision-making, it has been shown that NPV leads to better decisions than other indices [29]. For this reason, NPV is selected as the primary ranking criteria to find the optimal configuration, which is the most profitable case (i.e., that with the highest NPV). In the case where there are alternative configurations which produce the same benefits and returns, the other secondary metrics will need to be evaluated. LCC is a measurement of all costs incurred during a project's lifetime. BCR is defined as the ratio of the present value to the initial installation cost as calculated in Equation (18).

$$NPV = \sum_{n=0}^{N} \frac{F_{ATCF,n}}{(1+d_{nom})^n} \tag{16}$$

$$LCC = \sum_{n=0}^{N} \frac{F_{ATC,n}}{(1+d_{nom})^n} \tag{17}$$

$$BCR = \frac{NPV + C_{install}}{C_{install}} \tag{18}$$

The SPB of a project is determined as the number of years it takes before the cumulative forecasted cash flow equals or exceeds the initial investment. It can be expressed as the first point in the project's lifetime at which:

$$\sum_{n} F_{ATCF} \geq C_{install} \tag{19}$$

Figure 2 presents the microgrid design process using MDSTool, which is divided into two main sections: (1) Problem formulation and (2) simulation and analysis. In the first section, definitions of the design objective and the DER search space are decisive steps. The objective of a microgrid design must be clearly defined because it will decide which evaluation parameters will be used to search for the optimal configuration. In this case study, the design objective function is to maximize the economic benefits, therefore, NPV is used for the optimal DER sizing analysis. The search space in which the optimal DER capacity is located includes all of the possible capacities of the selected DERs considering associated technical and financial constraints. For example, the rated power of PV systems is typically constrained by the available installation space, especially for campus microgrids where PV modules are often installed on the rooftops of buildings [16]. MDSTool will perform the system operation optimization to find the optimal design for further analysis.

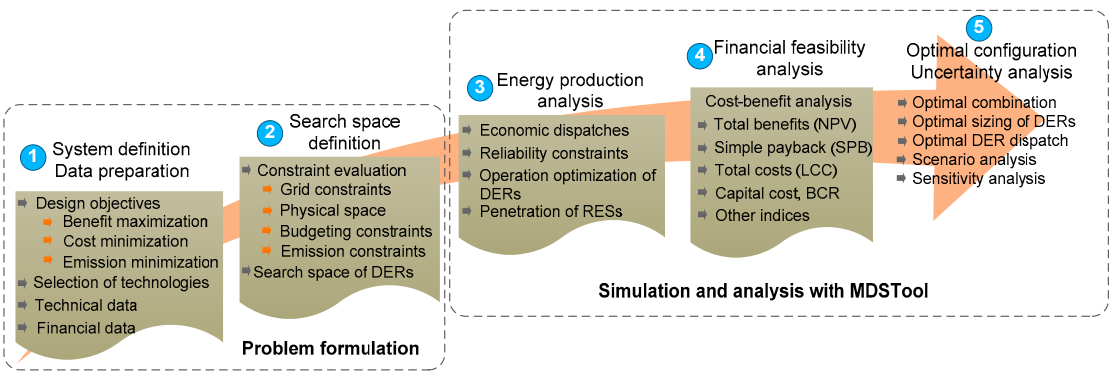


**Figure 2.** Microgrid design process with MDSTool.

## 3. Case Study of a Campus Microgrid in California, U.S.

The presented design method using MDSTool was applied to determine the optimal design for a university campus microgrid in California, U.S. The microgrid configuration, shown in Figure 3, comprises of a PV, an ESS using lithium-ion batteries and an FC. The microgrid is connected to the San Diego Gas and Electric (SDG&E) utility, and it is designed to power a high school, a university dormitory and a research building. This section analyzes all the data required to run this case study in MDSTool.

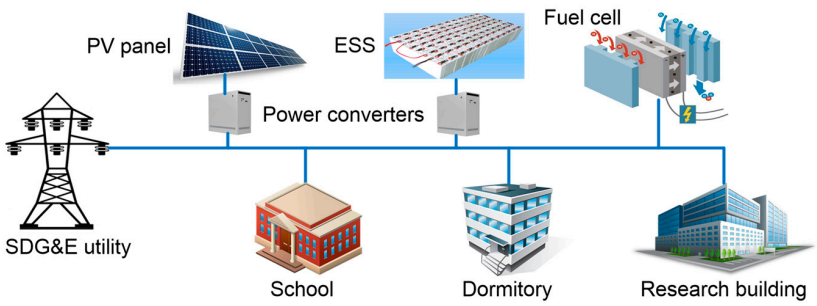


**Figure 3.** The campus microgrid architecture.

### 3.1. Electric Tariff

The applied electric tariff is AL-TOU of SDG&E utility, which is applicable to all metered non-residential customers, whose monthly maximum demand equals, exceeds, or is expected to equal or exceed 20 kW. This rate structure employs time-of-use (TOU) energy charges in \$/kWh and a monthly demand charge of 24.51 \$/kW [30]. The AL-TOU tariffs for November–April and May–October, and for weekdays/weekends are shown in Figure 4. The numbers in blue indicate the rates presented in Table 1, with the highest rate of 0.11703 \$/kWh and the lowest rate of 0.07745 \$/kWh [30]. There are no peak and off-peak hours during the weekend. Notably, the first six hours and the last hour of each weekday are the periods with the lowest power prices. This influences the selection of an appropriate dispatch algorithm for the ESS to benefit from the AL-TOU tariff. In addition, the very high monthly demand charge of 24.51 \$/kWh highlights the potential profit that can be generated by reducing demand charge via the microgrid.

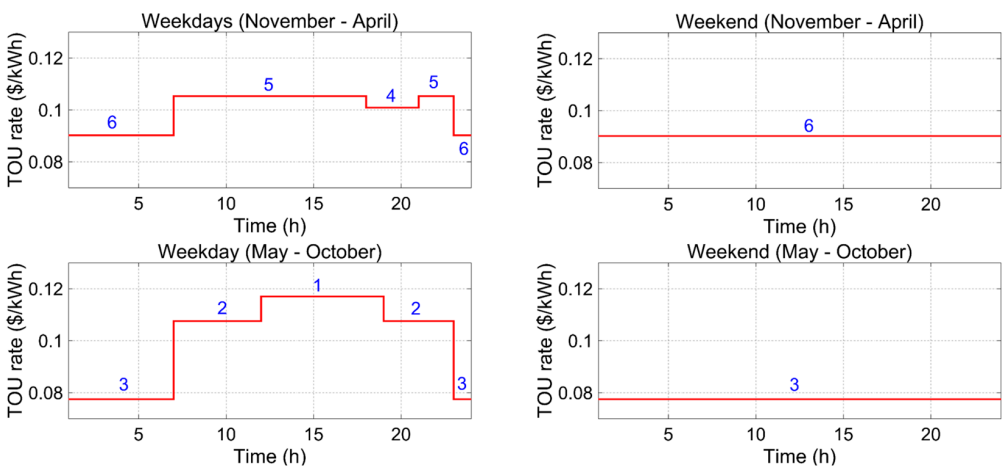


**Figure 4.** Time-of-use (TOU) electricity prices of SDG&E AL-TOU tariff.

**Table 1.** The rates of SDG&E AL-TOU tariff.

| Rate | 1 | 2 | 3 | 4 | 5 | 6 |
|---|---|---|---|---|---|---|
| Price (\$/kWh) | 0.11703 | 0.10756 | 0.07745 | 0.10088 | 0.10536 | 0.09025 |

### 3.2. Electricity Load Demand

In this study, the economic benefit of DSM is evaluated because it would substantially improve the economic security of the microgrid. To achieve this, two load profiles were created, including the base load and the controlled load. The system base load is assumed to be the existing load profile, whereas the controlled load is the expected load profile after applying load control, which results in the overall load reduction and load shifting.

#### 3.2.1. Base Load Data Generation

The electricity demand data for the three institutions attached to the microgrid—Preuss school, a dormitory for graduate students, and a research building called California Institute for Telecommunications and Information Technology, all located in the University of California, San Diego—were measured for three months (May, June, and July 2017). Based on these onsite measurement data, load profiles for an entire year, with a resolution of one hour, were generated for each type of load with the following assumptions: The load shape of each building is conserved by scaling the measured data; the total load reaches a maximum in March and September and a minimum in January and December; and the maximum, average, and minimum loads of the overall load profile are 1011 kW, 572 kW, and 247 kW, respectively. Table 2 summarizes the load parameters of each load type. Notably, the maximum and minimum loads of the total demand are different from the summation of the individual values because the maximum and minimum values of the three loads can occur at different times on any given day. Figures 5 and 6 show the typical daily load profiles and the total energy seasonal variations, respectively, of the electricity demands of the three loads. Figure 7 presents the total hourly electricity demand for a complete year.

**Table 2.** Load parameters.

| Building | Max. Load (kW) | Average Load (kW) | Min. Load (kW) | Load Factor |
|---|---|---|---|---|
| Dormitory | 439 | 213 | 74 | 0.49 |
| Research building | 404 | 249 | 133 | 0.62 |
| School | 324 | 110 | 37 | 0.34 |
| Total | 1011 | 572 | 247 | 0.57 |

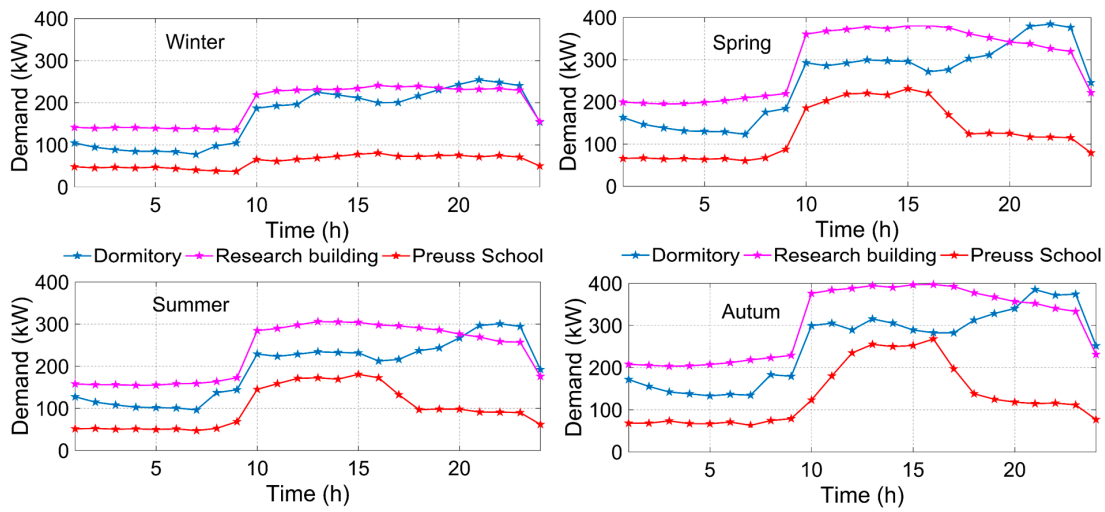


**Figure 5.** Typical daily load profiles in different seasons.

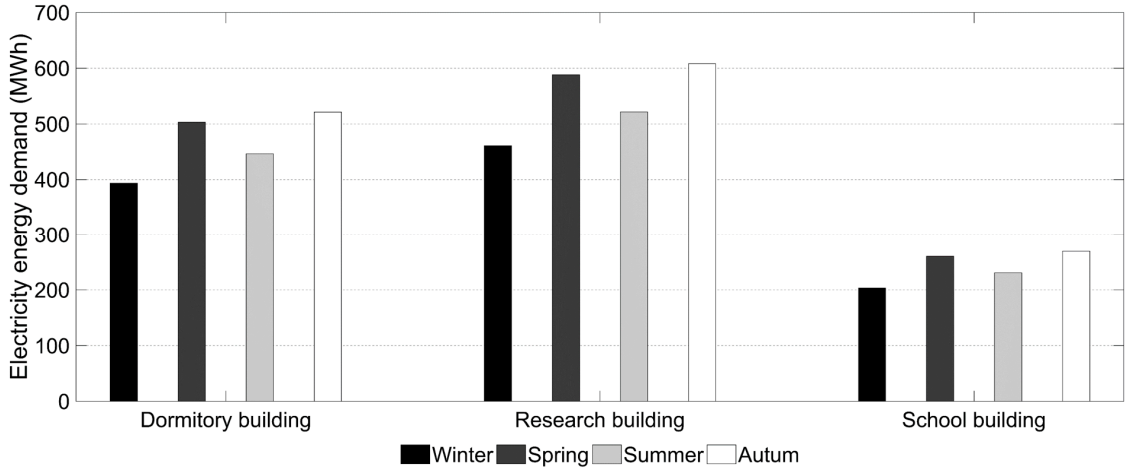


**Figure 6.** Seasonal variation in energy demand.

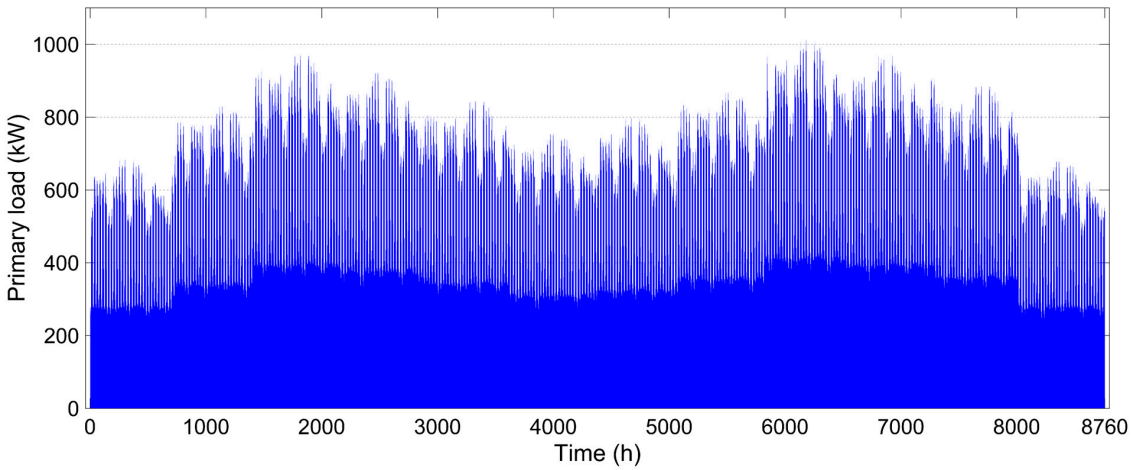


**Figure 7.** Hourly annual electricity demand.

One of the important parameters of the total load demand is its high load factor of 0.57. This means that the difference between the average and peak load is relatively low. The high load factor significantly influences the selection of the appropriate dispatch strategy and optimal sizing of the DER units, because a substantial proportion of the electricity savings generated by the microgrid deployment comes from energy charges rather than demand charges.

### 3.2.2. Controlled Load with DSM

The concept of DSM is executed by installing smart sensors, lighting control systems (LCS), electric heat pumps (EHP), and building energy management systems (BEMS). Details of DSM operation are not presented in this paper, but the associated latter assumptions and installation costs are based on the measurement data obtained from our previous microgrid project, the Internet-of-Things (IoT)-based campus microgrid at Seoul National University (SNU), South Korea, with a peak load of 912 kW [22].

DSM contributes to overall demand reduction and demand shifting, which shifts a portion of the load from periods with peak electricity prices to those with lower prices. Based on the performance of the SNU microgrid, the assumptions of load control with DSM for this study were established. The total demand was reduced by 8.9%, and 5% of the load from 11:00 a.m. to 05:00 p.m. was uniformly shifted to the period from 00:00 a.m. to 06:00 a.m. every weekday because this period has the lowest electricity prices. The demand over the weekend was not shifted. The load profile created from the base load data using these assumptions is defined as the controlled load.

### 3.3. Weather Resources

The data of the average Global Horizontal Irradiance (GHI), and temperature at the University of California, San Diego, was downloaded from the NASA Surface Meteorology and Solar Energy website [31]. Based on this data, 8760-h time-series data was generated to be used for simulations in MDSTool. Figure 8 presents the GHI over a complete year by hour.

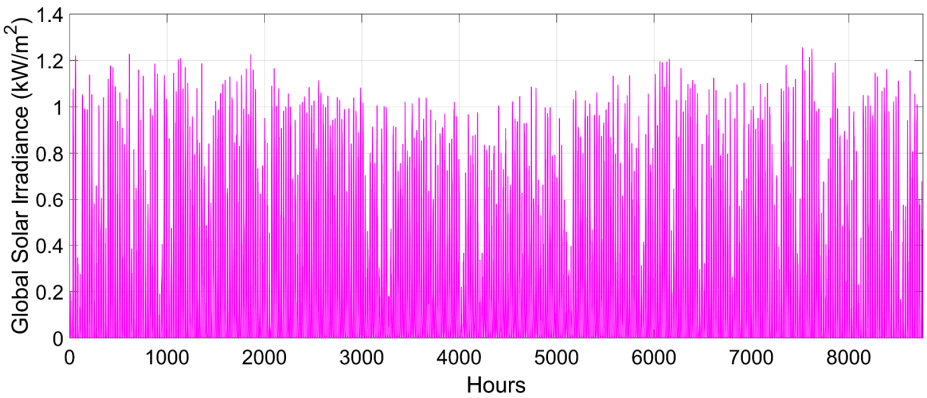


**Figure 8.** Annual Global Horizontal Irradiance (GHI) at the University of California San Diego.

### 3.4. Renewable Energy Incentives

To evaluate the financial feasibility of the microgrid project, all of the applicable incentives and tax credits were analyzed in this study. California's Renewables Portfolio Standard requires Californian electric utilities to have 33% of their retail sales derived from eligible renewable energy resources by 31 December 2020, 40% by 31 December 2024, 45% by 31 December 2017, and 50% by 31 December 2030 and all subsequent years [32]. This standard is one of the major factors driving the establishment of various state incentives for renewable energy projects, which are the main motivation of this paper.

The campus microgrid is eligible to receive federal tax credit and PTE on its PV system, and IBI under California self-generation incentive program (SGIP) for its ESS and FC. Other incentives considered include NEM and MACRS. Table 3 summarizes the incentives available in San Diego, California. Notably, the feed-in tariff, which is renewable market adjusting tariff (ReMAT), is applicable in California. However, according to the ReMAT policy, any customer who sells power to the utility under this tariff cannot participate in other state incentive programs [33]. In this case, if the microgrid project were to be enrolled under ReMAT, it would not be eligible for the SGIP, NEM, and PTE programs. For this reason, the incentive programs described in Table 3 were analyzed and included in the project financial analysis.

**Table 3.** Incentives and tax credits related to microgrid technologies in California.

| Name | Implementing Sector | Category | Incentive Type | Amount |
|---|---|---|---|---|
| Business Energy Investment Tax Credit [34] | Federal | Financial incentive | Corporate tax credit | 30% for solar systems |
| Self-Generation Incentive Program [35] | California | | | |
| Advanced energy storage | | Financial incentive | Rebate program | 0.22 $/Wh |
| Fuel cell | | Financial incentive | Rebate program | 1.0 $/W |
| Net Energy Metering [36] | California | Regulatory policy | Net metering | Excess generation sold at retail TOU rate |
| Modified Accelerated Cost-Recovery System [37] | Federal | Financial incentive | Corporate depreciation | 5-year accelerated depreciation |
| Property Tax Exclusion for Solar Energy Systems [38] | California | Financial incentive | Property tax incentive | 100% of system value |

### 3.4.1. Business Energy Investment Tax Credit

Energy tax credits for renewables substantially enhance after-tax cash flow and promote an investment. An energy ITC is calculated as an immediate reduction in income taxes equal to a percentage of the installed cost of a new investment. The ITCs for solar and FC technologies are summarized in Table 4, wherein the specified date is the expiration date in each year [34]. Notably, the expiration date for solar technologies is based on when the project construction starts. The ITC for PV systems remains constant at 30% until December 2019, after which it will progressively reduce to 10% from 2022 onward, with no maximum credit, whereas the ITC for FCs ended in 2016 [34]. The PV system components eligible for the ITC include the ESS and the power conditioning system.

**Table 4.** Business energy investment tax credit.

| Technology | 12 Dec. 2016 | 12 Dec. 2017 | 12 Dec. 2018 | 12 Dec. 2019 | 12 Dec. 2020 | 12 Dec. 2021 | 12 Dec. 2022 | Future Years |
|---|---|---|---|---|---|---|---|---|
| PV, Solar Water Heating, Solar Space Heating/Cooling, Solar Process Heat | 30% | 30% | 30% | 30% | 26% | 22% | 10% | 10% |
| Fuel Cells | 30% | N/A | N/A | N/A | N/A | N/A | N/A | N/A |

### 3.4.2. California Self-Generation Incentive Program

SGIP is available to the customers of four utilities in California: SDG&E, Pacific Gas and Electric, Southern California Edison, and Southern California Gas (SoCal Gas). The objective of this incentive program is to encourage the installation of new and sustainable technologies, thereby contributing to a reduction of greenhouse gases, demands, and customer electricity purchases. SGIP provides financial incentives, which are in the form of IBIs, to customers of the aforementioned utilities who generate electricity with wind turbines, FCs using renewable and non-renewable fuels, various forms of combined heat and power, and advanced energy storage. The incentive rates of SGIP for FCs and ESSs are detailed in Tables 5 and 6, respectively [35].

In a year, the total SGIP fund is divided into incentive steps that differ in their incentive rates. The availability of funding steps depends on the number of projects that have applied for this incentive. In the situation where there are many projects, if the funding of a step ends, the next step will be opened with lower incentive rates. For FC technology, the total generation incentive fund is divided into three steps, and the incentive rates decrease by 0.1 $/W between each step. For energy storage, the total incentive fund is divided into five steps. The reduction in incentive rates based on energy storage capacity and generation capacity are shown in Tables 7 and 8, respectively [35]. Energy storage incentives are available for up to the storage capacity of 6 MWh, and FC incentives are paid for up to 3 MW both with tiered incentive rates. The SGIP incentive rates of the last funding step, which are the lowest values, were included in the economic model of MDSTool so that the results were more conservative. Variations in the SGIP rates were evaluated in the sensitivity analysis.

**Table 5.** Generation incentive rates per Watt for fuel cell (FC) in SGIP.

| | Step 1 ($/W) | Step 2 ($/W) | Step 3 ($/W) |
|---|---|---|---|
| FC (Electric Only) | 1.20 | 1.10 | 1.00 |

**Table 6.** Energy storage incentives per Watt-hour in SGIP.

| Technology | Step 1 ($/Wh) | Step 2 ($/Wh) | Step 3 ($/Wh) | Step 4 ($/Wh) | Step 5 ($/Wh) |
|---|---|---|---|---|---|
| Large Storage Claiming ITC | 0.36 | 0.32 | 0.29 | 0.25 | 0.22 |

**Table 7.** Incentive declines based on energy storage capacity in SGIP.

| Energy Storage Capacity | Incentive Rate as Percentage of Base |
|---|---|
| 0–2 MWh | 100% |
| Greater than 2 MWh to 4 MWh | 50% |
| Greater than 4 MWh to 6 MWh | 25% |

**Table 8.** Incentive declines based on generation capacity in SGIP.

| Generation Capacity | Incentive Rate as Percentage of Base |
|---|---|
| 0–1 MW | 100% |
| Greater than 1 MW to 2 MW | 75% |
| Greater than 2 MW to 3 MW | 50% |

#### 3.4.3. Net Energy Metering

Residential and commercial customers of SDG&E whose electricity generating systems supply their onsite electricity demand in full or partly using solar, wind, biomass, geothermal, or small hydro are eligible for the NEM program of California. NEM provides customers full retail rate credits for any excess power generated by their system that enters the grid [36]. In this case study, the abovementioned AL-TOU tariff is applied to NEM. Participation in NEM does not restrict a customer's eligibility for any other rebate, incentive, or credit provided by an electric utility [36].

#### 3.4.4. Modified Accelerated Cost-Recovery System

For tax purposes, depreciation is a means of recovering, through an income tax deduction, the cost of property used in a trade or business, or of property held for the production of income. Under modified accelerated cost-recovery system (MACRS), the project may recover investments on a certain property through depreciation deductions. In this case study, the FC and the PV system, including the ESS, are eligible for five-year MACRS [37]. The depreciation rates for recovery periods from the first year to the sixth year are 20.00%, 32.00%, 19.20%, 11.52%, 11.52%, and 5.76%, respectively [37].

#### 3.4.5. Property Tax Exclusion for Solar Energy System

Section 73 of the California Revenue and Taxation Code allows property tax exclusion (PTE) for active solar energy systems installed between 1 January 1999 and 31 December 2024 [38]. An active solar energy system is defined as a system that uses solar devices, which are thermally isolated from the living space or any other area where the energy is used, to facilitate the collection, storage, or distribution of solar energy. Such a system contains storage devices, power conditioning equipment, transfer equipment, and components related to the functioning of these items. The systems that qualify for this incentive include solar space conditioning systems, solar water heating systems, photovoltaic systems, solar thermal electric systems and solar mechanical energy. Solar swimming pool heaters, hot tub heaters, passive energy systems and wind energy systems are not eligible for this incentive. An active solar energy system does not contain any auxiliary equipment that uses a source other than solar energy to provide usable energy. In this case study, the PV system, including the ESS and converter, is eligible for 100% exclusion [38].

### *3.5. Component Parameters and Financial Parameters*

The input data of component parameters and the project financial parameters are detailed in Tables 9 and 10, respectively. The capital costs of DERs vary widely depending on many factors such as the manufacturer, rated capacity, market regulations, and technical features. The project financial parameters include a high level of uncertainty as they depend on the local economy. For the present study, the nominal discount rate was assumed to be 8% [16]. The expected inflation rate of

2.15% was the average value of the historical U.S. consumer price index over the previous 20 years. For commercial ownership, the project was assumed to be 100% financed by a long-term loan.

**Table 9.** Parameters of distributed energy resource (DER) technologies.

| Technology | Cost | Value | Unit |
|---|---|---|---|
| PV [16] | Capital cost | 2390 | $/kW |
| | O and M cost | 10 | $/kW/y |
| | Life time | 25 | y |
| ESS [16] | Capital cost | 350 | $/kWh |
| | Replacement cost | 300 | $/kWh |
| | O and M cost | 5 | $/kWh/y |
| | Throughput | 3000 | kWh/unit |
| | Round-trip efficiency | 90 | % |
| FC [39] | Capital cost | 4000 | $/kW |
| | Replacement cost | 2500 | $/kW |
| | O and M cost | 0.01 | $/kW/h |
| | Life time | 40000 | h |
| | Fuel curve slope | 0.21 | L/kWh |
| | Fuel price | 0.3 | $/L |
| Converter | Capital cost | 250 | $/kW |
| | Replacement cost | 250 | $/kW |
| | O and M cost | 0 | $/kW/y |
| | Life time | 15 | y |
| | Efficiency | 95 | % |
| DSM | Capital cost | 440,000 | $ |

**Table 10.** Project financial data.

| | Parameter | Value | Unit |
|---|---|---|---|
| Financial parameters | Nominal discount rate | 8 | % |
| | Expected inflation rate | 2.15 | % |
| | Project lifetime | 25 | y |
| Taxes and insurance | Federal income tax rate | 30 | % |
| | California income tax rate | 8.84 | % |
| | Property tax rate | 2 | % |
| | Annual insurance | 0.5 | % |
| Project debt | Debt size | 100 | % |
| | Loan term | 25 | y |
| | Loan rate | 7.5 | % |
| Depreciation | Depreciation system | MACRS | - |
| | Depreciation term | 5 | y |

## 4. Results and Analysis

### 4.1. Optimal Configuration

As described above in the microgrid architecture, the campus microgrid may comprise of a PV, an FC, or an ESS. As such, this study considered two options: "PV + ESS" and "PV + FC + ESS". The optimal design for each of these options was determined and compared to select the optimal microgrid configuration. The energy production and consumption of the two microgrid configurations were compared to that of the base case, which is assumed to be the existing system wherein the entire load demand is supplied by the SDG&E utility. In addition, to evaluate the economics of load control, the base load was used to simulate the base case, while the microgrid cases were simulated using the controlled load. To simulate the case study in MDSTool, in addition to the input data presented above, a search space must be defined to locate the optimal configuration. The search space of PV ranged from 0 to 300 kW, that of ESS ranged from 0 to 1000 kWh and that of its converter ranged from 0 to 500 kW, all in steps of 25 kW. The rated power of FC was constrained by the total capital cost.

The energy outputs of the PV + ESS and PV + FC + ESS microgrid configurations are illustrated in Figures 9 and 10, respectively. In both cases, the ESS was operated by a peak-shaving dispatch strategy, which discharges the ESS during peak-load periods and charges the ESS in periods with low electricity rates to reduce monthly demand charges. Specifically, with the AL-TOU tariff, the ESS charges during the first six hours of a day and discharges to flatten grid purchases as shown in the two figures. The period of high power demand in a day often coincides with the on-peak utility billing period. In the PV + FC + ESS configuration, the FC operates at full power to cover a proportion of the total load, while the rest of the load is supplied by the PV, utility, or ESS discharge. This operation of FC resulted in significant energy savings.

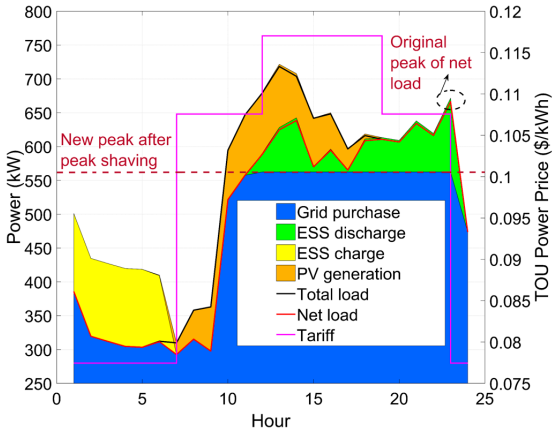


**Figure 9.** Energy outputs on a typical day in the PV + ESS configuration.

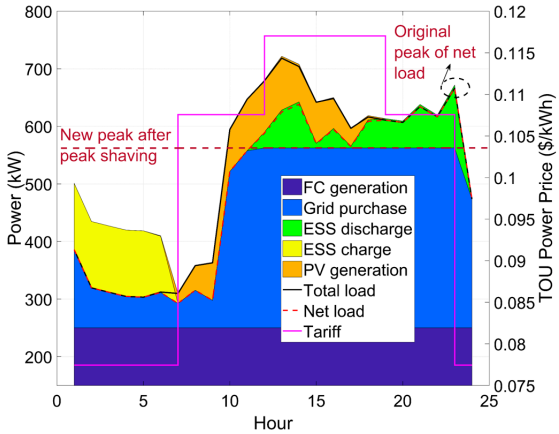


**Figure 10.** Energy outputs on a typical day in the PV + FC + ESS configuration.

Table 11 details the breakdown of energy production and electricity charges of the two optimal microgrid configurations compared to the base case. In the base case, the total annual energy charge is \$489,584.94, whereas the annual demand charge is \$250,996.72, which constitutes more than half of the energy charge. The noticeably high annual demand charge is partly owing to the high monthly demand charge levied by the AL-TOU tariff, which is 24.51 \$/kW.

**Table 11.** Sizing and energy analysis of optimal configurations.

| Parameter | Unit | Base Case | Optimal PV + ESS | Optimal PV + FC + ESS |
|---|---|---|---|---|
| **Sizing of DERs** | | | | |
| FC rated power | kW | - | - | 220 |
| PV rated power | kW | - | 300 | 50 |
| ESS rated capacity | kWh | - | 625 | 300 |
| Converter | kW | - | 150 | 75 |
| **Energy production** | | | | |
| Annual grid purchase | kWh/y | 5,007,087.01 | 3,939,737.47 | 2,467,258.58 |
| Grid fraction | % | 100.00 | 87.38 | 54.96 |
| Annual PV production | kWh/y | - | 569,055.20 | 94,842.53 |
| PV fraction | % | - | 12.62 | 2.11 |
| Annual FC production | kWh/y | - | - | 1,927,200.00 |
| Annual fuel cost | $/y | - | - | 121,413.60 |
| FC fraction | % | - | - | 42.93 |
| Electricity charge | | | | |
| Annual energy charge | $/y | 489,584.94 | 378,943.16 | 242,823.93 |
| Annual demand charge | $/y | 250,996.72 | 180,946.86 | 133,320.26 |
| Annual electricity savings | $/y | 0 | 180,691.64 | 364,437.47 |

With the optimal PV + ESS configuration supplying the controlled load, the annual energy charge and demand charge were reduced to $378,943.16 and $180,946.86, respectively, resulting in the annual electricity saving of $180,691.64. In the PV + FC + ESS configuration, the annual energy and demand charges were reduced further because a significant proportion of the grid purchase was replaced by the FC generation. Indeed, the annual energy charge and demand charge were greatly curtailed to $242,823.93 and $133,320.26, respectively, leading to annual electricity savings of up to $364,437.47 (49.21%). However, an amount of $121,413.60 needed to be paid for annual fuel cost in this case.

Table 12 compares the financial feasibility of the two optimal microgrid cases, and a breakdown of their associated costs and benefits is illustrated in Figure 11. The capital cost of PV + ESS configuration was $1,275,750.00, and this cost was used as a constraint on the investment size when determining the optimal PV + FC + ESS configuration in order to establish which configuration had the higher profitability. The PV + FC + ESS case received more grant incentives because both the FC and the ESS are eligible for the SGIP. With approximately the same capital costs, the PV + FC + ESS configuration produced an NPV of $1,594,000.00, which is $528,800.00 higher than that of the PV+ESS configuration. This leads to a notable difference in the resulting BCRs. The PV + FC + ESS configuration has a BCR of 2.25, while the other has a BCR of just 1.84. Both cases have an SPB of around 5 y. Based on this comparison, it was concluded that the financial performance of PV + FC + ESS configuration is superior to that of the PV + ESS configuration. As a result, the PV + FC + ESS microgrid with the FC of 220 kW, PV of 50 kW, and ESS of 300 kWh was selected as the optimal microgrid configuration for the sensitivity analysis.

**Table 12.** Financial performance of the optimal microgrid configurations.

| Financial Feasibility | Unit | Optimal PV + ESS | Optimal PV + FC + ESS |
|---|---|---|---|
| **Capital cost** | $ | 1,275,750.00 | 1,277,250.00 |
| **Incentives** | | | |
| SGIP | $ | 137,500.00 | 286,000.00 |
| ITC | $ | 250,725.00 | 185,175.00 |
| Property eligible for PTE | $ | 835,750.00 | 617,250.00 |
| **Financial metrics** | | | |
| NPV | $ | 1,065,200.00 | 1,594,000.00 |
| SPB | y | 4.92 | 5.20 |
| BCR | - | 1.84 | 2.25 |

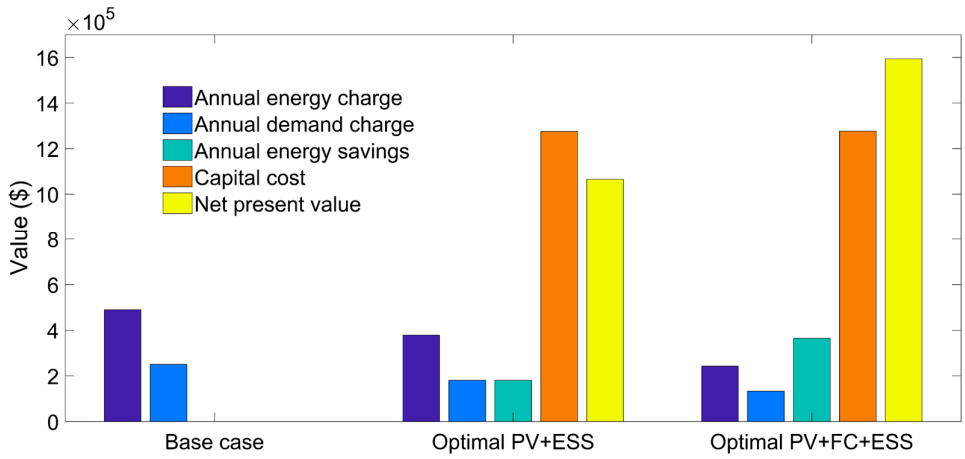


**Figure 11.** Breakdown of the costs and benefits for microgrid configurations.

## *4.2. Sensitivity Analysis*

### 4.2.1. Incentives

As described in the SGIP section, the incentive rates for the ESS and FC vary according to predetermined incentive steps, and this variation is considered in this section. The SGIP rate for large storage units claiming ITC declines from 0.36 $/Wh to 0.22 $/Wh, and that for the FC decreases by 0.1 $/W between incentive steps. As presented in Table 4 with regards to the ITC for PV systems, the incentive rate will be adjusted in the future. PV projects can obtain an ITC of 30% if construction starts before 12 December 2019, after which the rate will decrease by 4% each year until 12 December 2021 and remain at 10% thereafter. In addition to these considerations, the scenarios without each of the ITC, SGIP, or PTE, and a scenario without all the three incentives were simulated to examine their impact on the financial feasibility of the optimal configuration and the sizing of DERs.

Table 13 presents the impact of variation in incentive levels and their absence on the financial indices of the optimal configuration. It is apparent that the higher the incentive rates, the more profitable the project becomes, with a higher NPV and a smaller SPB. For the ITC, the project construction should start soon to obtain a higher ITC value. When the ITC declines to 10%, the NPV will decrease by $76,800.00. The SGIP strongly enhances the financial feasibility of the microgrid. In the situation where both the FC and ESS can receive the highest SGIP rates, the optimal configuration produces an NPV of up to $1,721,600.00, with the SPB decreasing to 4.03 y. Of the three incentives, the PTE slightly affects the project's NPV when it is not applied. In contrast, the absence of the SGIP has dominant influences. Most importantly, if all of the three incentives are removed, the microgrid's SPB will be more than 7 y and its NPV will decrease by nearly half, which takes the BCR down to just 1.54.

Table 14 presents the impact of excluding incentives on the optimal sizing of the DERs. It can be seen that the removal of tax credits (ITC and PTE) have a slight impact on the DER sizing. When the ITC and PTE are excluded, the capacity of the ESS and PV slightly decreases. This is because both the ITC and PTE are applicable only to the ESS and PV in the configuration. This indicates that the incentives which are designed for a specific technology will increase the penetration of that technology in microgrid systems. The SGIP has a decisive impact on the optimal DER mix. When the SGIP is removed, the FC becomes infeasible, the ESS capacity decreases, and the financial indices are notably worse than that of the optimal PV + ESS configuration. This is because the SGIP provides a significant amount of IBIs, which helps to reduce the installation costs of FC and ESS. This evidence provides insights into the economic importance of renewable energy incentives for microgrid project investment, and they should therefore be included in the design and planning process for microgrids.

**Table 13.** Impact of the variation in incentives and their absence on financial feasibility.

| Incentive | | Financial Metrics of Optimal PV + FC + ESS | | |
|---|---|---|---|---|
| | | NPV ($) | SPB (y) | BCR |
| **Incentive Variations** | | | | |
| ITC | 26% | 1,574,700.00 | 5.28 | 2.23 |
| | 22% | 1,555,500.00 | 5.37 | 2.22 |
| | 10% | 1,497,900.00 | 5.62 | 2.17 |
| SGIP for ESS | 0.36 $/Wh | 1,619,500.00 | 5.12 | 2.31 |
| | 0.32 $/Wh | 1,616,400.00 | 5.13 | 2.30 |
| | 0.29 $/Wh | 1,611,700.00 | 5.16 | 2.28 |
| | 0.25 $/Wh | 1,601,600.00 | 5.18 | 2.26 |
| SGIP for FC | 1.20 $/W | 1,696,100.00 | 4.44 | 2.38 |
| | 1.10 $/W | 1,645,000.00 | 5.04 | 2.31 |
| SGIP: 0.36 $/Wh for ESS and 1.2 $/W for FC | | 1,721,600.00 | 4.03 | 2.44 |
| **Incentive excluded** | | | | |
| ITC | | 1,449,800.00 | 5.82 | 2.14 |
| PTE | | 1,570,100.00 | 5.24 | 2.23 |
| SGIP | | 1,027,600.00 | 6.94 | 1.66 |
| ITC + SGIP + PTE | | 838,860.00 | 7.74 | 1.54 |

**Table 14.** Impact of the absence of incentives on DER sizing.

| Incentive Excluded | ITC and PTE | SGIP |
|---|---|---|
| **Incentive Considered** | **SGIP, NEM, MACRS** | **ITC, PTE, NEM, MACRS** |
| **Optimal Sizing** | | |
| FC (kW) | 240 | 0 |
| PV (kW) | 25 | 300 |
| ESS (kWh) | 250 | 275 |
| Converter (kW) | 75 | 75 |
| **Financial Metrics** | | |
| NPV ($) | 1,475,300.00 | 992,170.00 |
| SPB (y) | 5.81 | 5.09 |
| Capital Cost ($) | 1,271,000.00 | 1,272,000.00 |
| BCR | 2.16 | 1.78 |

#### 4.2.2. Uncertain Financial Parameters

The project financial parameters and the capital costs of DER technologies can vary considerably because they depend on the status of local economy, manufacturers, and technical characteristics. The impact of this uncertainty on the NPV and SPB are examined in this section. Capital costs were altered by between −50% and 50% to reflect existing prices and the downward trend in prices of DERs due to technological innovation. The financial parameters were varied from −25% to 25% because the state of local economy may go up or down. The results of the sensitivity analysis for parameter uncertainty are presented in Figures 12 and 13.

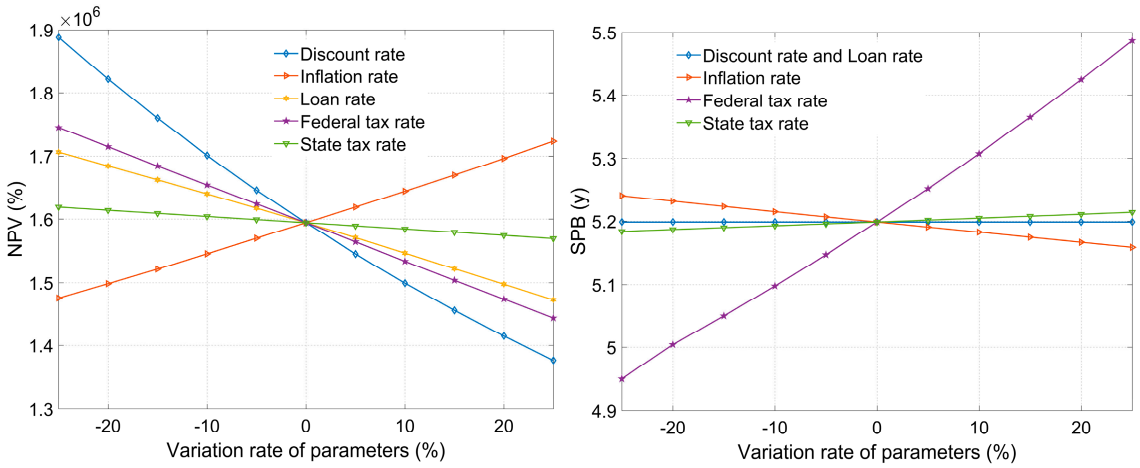


**Figure 12.** Impact of financial parameter variation on the NPV and SPB.

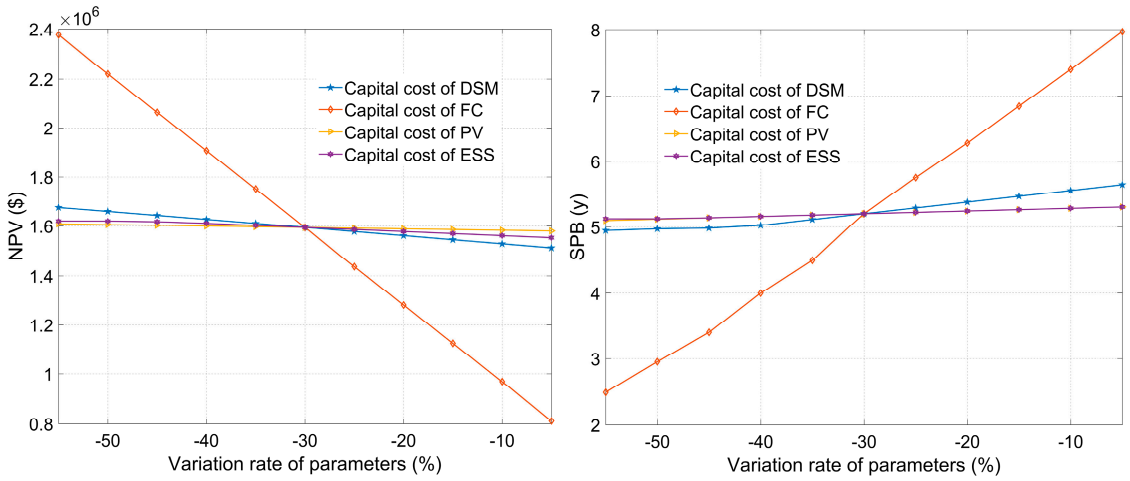


**Figure 13.** Impact of capital cost variation on the NPV and SPB.

Of the financial parameters, only the inflation rate has a positive influence on the NPV, and the discount rate is the most sensitive. When the discount rate is decreased by 25%, the NPV goes up to $1,887,900.00, while it is $1,376,000.00 if the discount rate is increased by 25%. The loan rate and federal tax rate are the next most sensitive parameters. Compared to the federal tax rate, the state tax rate has a slightly negative impact on the NPV because its nominal value is just 8.84%. When changing from −25% to 25%, the federal tax rate makes the SPB vary from 4.95 to 5.49 y, while the discount and loan rates have no impact on the SPB. The SPB changes marginally around 5.20 y corresponding to variations in the inflation rate and state tax rate.

In terms of capital costs, it is observed that this cost of FC dominantly affects both the NPV and SPB. When the capital cost of FC is increased by 50%, the NPV sharply decreases to $811,340.00, with the SPB rising up to 7.97 y. When it is reduced by 50%, the project is noticeably profitable, with an NPV of $2,376,600.00 and an SPB of only 2.50 y. This can be ascribed to the operation of FC, which results in most of the electricity savings by the microgrid deployment. The next most sensitive capital cost is that of DSM. The costs of ESS and PV have a slight impact, which is owing to their small capacity in the optimal configuration. These sensitivity results illustrate that investment in microgrids will be more financially attractive in the future if the installation costs of DERs continue to fall and more renewable energy incentives are provided by governments or utilities.

The analysis performed above for the university campus microgrid validates the advantages of the proposed microgrid design method using MDSTool. Compared to previous studies, the design approach can evaluate the financial feasibility of a whole microgrid project, rather than of a single DER

technology. The techno-economic analysis incorporates the economic benefits from various incentives and tax credits for renewable energy technologies. The problem of optimal mix and sizing of DERs can be solved by defining the design objective function. The results from MDSTool help to intensively evaluate the technical and economic efficiency of a hybrid microgrid system, including the operational efficiency of each energy generation or storage unit, and the performance of an economic dispatch strategy. In addition, the results provide multiple economic measures such as NPV, LCC, SPB, and BCR, which offer various criteria that can be designed for the problem of optimal design. For instance, if an investor requires a minimum period to recover the initial investment capital, SPB will be used as the primary benchmark to select the optimal microgrid configuration. In another case when a microgrid owner asks for a configuration with minimum operating costs, LCC will be selected as the design objective. Therefore, the significance of the proposed methodology is that it can be generalized to different microgrid design problems.

The sensitivity analysis arising from the presented microgrid design process provides a means to examine the importance and influence of incentives on the optimal design. Moreover, this analysis is also helpful for renewable energy policy makers. Indeed, it helps them determine what extent an incentive program or a combination of various types of incentive is effective for promoting more investment in microgrid projects. Based on the results, a policy maker can decide incentive rates, applicable durations, and other incentive strategies which are appropriate for short-term and long-term promotion of renewable energy systems. To increase the penetration of a particular technology, the government or the utility should launch an incentive program specifically designed for that technology with a certain level of incentive rate. Similarly, to promote a specific microgrid configuration, one or more incentive programs should be available to the DERs in that configuration, and a microgrid is eligible for the incentives if, and only if, the specified DERs are integrated together. Furthermore, a tiered structure for incentive rates, which is based on construction time of a microgrid and/or rated capacity of technologies, can be used to encourage the microgrid implementation in certain periods, as well as to support a certain scale of microgrids, such as buildings, campuses or residential areas.

## 5. Conclusions

This paper presented a design method for commercial microgrids using MDSTool, which was applied to determine the optimal design for a university campus microgrid. The optimal microgrid configuration was obtained based on financial feasibility analysis considering various renewable energy incentives. With the objective of maximizing profitability by microgrid deployment, incentives and tax benefits were found to have a strong effect on the optimal microgrid design, including the optimal mix and sizing of DERs. In particular, investment-based incentives were found to have a decisive impact because they help to decrease the high installation costs of DERs, which has been the main challenge of integrating hybrid renewable energy systems. Therefore, it is concluded that accessing all associated incentives is crucial for effective microgrid design and planning.

The results of financial feasibility analysis are beneficial to different sectors such as utility, policy makers in renewable energy development, and industry. The California market was investigated as a case study, but the proposed method can be applied to any particular area with different market conditions and incentive policies. The results indicated that investment in microgrid in a market with diversity of incentives for DER technologies will be financially attractive to commercial investors. In some countries where there are few incentive programs for microgrids, or the penetration of RESs is inadequate, this study provides a reference for the government and utility to establish incentive policies for the adoption of more renewable energy systems. Recently, many countries have set their targets for renewable energy generation to significantly reduce emissions from the power sectors. This study highlights that financial incentives for DERs play an important role in achieving renewable and sustainable energy goals.

**Author Contributions:** Conceptualization, I.-Y.C.; Data curation, B.H.V.; Investigation, D.-J.W.; Methodology, M.H.; Resources, W.T. and T.N.; Supervision, I.-Y.C.; Writing–original draft, B.H.V.; Writing–review & editing, M.H.

**Funding:** This work was funded by the Korea Electric Power Corporation [Grant number: R18XA06-19] and the Ministry of Science and ICT, Korea, under the ITRC (Information Technology Research Center) support program (IITP-2018-0-01396) supervised by the IITP (Institute for Information & Communications Technology Promotion).

**Acknowledgments:** This work was supported by the Global Scholarship Program for Foreign Graduate Students at Kookmin University.

**Conflicts of Interest:** The authors declare no conflict of interest.

## Nomenclature

| | |
|---|---|
| *Acronyms* | |
| (B)ESS | (Battery) energy storage system |
| DERs | Distributed energy resources |
| DSM | Demand side management |
| FC | Fuel cell |
| IBI(PBI) | Investment/production-based incentive |
| ITC(PTC) | Investment/production tax credit |
| MACRS | Modified accelerated cost-recovery system |
| MDSTool | Microgrid Decision Support Tool |
| NEM | Net energy metering |
| PTE | Property tax exclusion |
| RESs | Renewable energy resources |
| SGIP | California self-generation incentive program |
| STC | Standard testing condition |
| TOU | Time-of-use |
| *Variables and parameters* | |
| $k$ | Rate constant of batteries [$h^{-1}$] |
| $c$ | Capacity ratio of batteries |
| $x$ | Fuel curve intercept coefficient of FC [L/kWh] |
| $y$ | Fuel curve slope of FC [L/kWh] |
| $t$ | Time step [h] |
| $r$ | Inflation rate [%/y] |
| $\phi_{pvd}$ | Property value declination rate [%/y] |
| $f_d$ | Debt fraction [%] |
| $d_{nom}$ | Nominal discount rate [%/y] |
| $\delta_s/\delta_f$ | State/federal tax rate [%] |
| $\delta$ | Effective tax rate [%] |
| $N$ | Project lifetime [y] |
| $N_R$ | Replacement years of DERs [y] |
| $P_{pv}$ | Output power of PV [kW] |
| $P_{pv,STC}$ | Rated power of PV at STC [kW] |
| $K_T$ | Temperature coefficient of PV power |
| $T_{cell}$ | PV cell temperature [°C] |
| $T_{STC}$ | Temperature at STC [°C] |
| $G$ | Solar irradiance at STC [$kW/m^2$] |
| $G_T$ | Solar irradiance incident on PV [$kW/m^2$] |
| $P_{\max d}$ | Maximum discharging power of batteries [kW] |

*Variables and parameters*

| | |
|---|---|
| $P_{\max c}$ | Maximum charging power of batteries [kW] |
| $Q_{\max}$ | Maximum capacity of batteries [kWh] |
| $P_r$ | Rated power of FC [kW] |
| $P_{gen}$ | Generated output power of FC [kW] |
| $P_{load}$ | Load demand [kW] |
| $P_G$ | Power generated by DERs and RESs [kW] |
| $P_g$ | Output power of generators [kW] |
| $P_S$ | Net output power of storage units [kW] |
| $P_{dch}$ | Discharging power of storage units [kW] |
| $P_{gbuy}$ | Power purchased from the utility [kW] |
| $P_{gsell}$ | Power sold to the utility [kW] |
| $SoC$ | State-of-charge of storage units [%] |
| $C_{total}$ | Total cost of supplying the dispatch power [$] |
| $C_{gen}$ | Cost of operating generators [$] |
| $C_{dch}$ | Cost of discharging storage units [$] |
| $C_{gbuy}$ | Cost of buying electricity from the utility [$] |
| $C_{gsell}$ | Revenue from selling electricity to the utility [$] |
| $C_{dres}$ | Revenue from demand response [$] |
| $C_{anc}$ | Revenue from ancillary services [$] |
| $C_{install}$ | Total installation cost [$] |
| $C_{annual}$ | Annual operating costs affected by inflation [$] |
| $C_{o\&m}$ | Operation and maintenance cost [$] |
| $C_{fuel}$ | Fuel cost [$] |
| $C_{ins}$ | Insurance cost [$] |
| $C_{rep}$ | Replacement cost [$] |
| $C_{prt}$ | Property tax [$] |
| $C_{emsp}$ | Emission penalty cost [$] |
| $C_{ibi}/C_{pbi}$ | Amount of IBI/PBI [$] |
| $C_{grev}$ | Grid revenues [$] |
| $C_{emsc}$ | Emission reduction credit [$] |
| $C_{salv}$ | Project salvage value [$] |
| $C_{debt}$ | Debt payment [$] |
| $C_{tax}$ | Income tax [$] |
| $C_{saving}$ | Energy savings [$] |
| $F_{in}/F_{out}$ | Pre-tax cash inflows/outflows [$] |
| $F_{PTC}/F_{ATC}$ | Pre-tax/after-tax cost [$] |
| $F_{PTCF}/F_{ATCF}$ | Pre-tax/after-tax cash flow [$] |
| $NPV$ | Net present value [$] |
| $LCC$ | Lifecycle cost [$] |
| $BCR$ | Benefit-cost ratio |
| $SPB$ | Simple payback period [y] |

## References


1. Husein, M.; Hau, V.B.; Chung, I.Y.; Chae, W.K.; Lee, H.J. Design and dynamic performance analysis of a stand-alone microgrid-A case study of Gasa Island, South Korea. *J. Electr. Eng. Technol.* **2017**, *12*, 1777–1788.
2. Arghandeh, R.; Woyak, J.; Onen, A.; Jung, J.; Broadwater, R.P. Economic optimal operation of Community Energy Storage systems in competitive energy markets. *Appl. Energy* **2014**, *135*, 71–80. [CrossRef]
3. Han, X.; Zhang, H.; Yu, X.; Wang, L. Economic evaluation of grid-connected micro-grid system with photovoltaic and energy storage under different investment and financing models. *Appl. Energy* **2016**, *184*, 103–118. [CrossRef]
4. Amir, V.; Jadid, S.; Ehsan, M. Optimal design of a multi-carrier microgrid (MCMG) considering net zero emission. *Energies* **2017**, *10*, 2109. [CrossRef]

5. Mazzola, S.; Astolfi, M.; Macchi, E. The potential role of solid biomass for rural electrification: A techno economic analysis for a hybrid microgrid in India. *Appl. Energy* **2016**, *169*, 370–383. [CrossRef]
6. Ou, T.C.; Hong, C.M. Dynamic operation and control of microgrid hybrid power systems. *Energy* **2014**, *66*, 314–323. [CrossRef]
7. Bui, V.H.; Hussain, A.; Kim, H.M. Optimal operation of microgrids considering auto-configuration function using multiagent system. *Energies* **2017**, *10*, 1484. [CrossRef]
8. Ou, T.C.; Lu, K.H.; Huang, C.J. Improvement of transient stability in a hybrid power multi-system using a designed NIDC (Novel Intelligent Damping Controller). *Energies* **2017**, *10*, 488. [CrossRef]
9. Howlader, A.M.; Matayoshi, H.; Sepasi, S.; Senjyu, T. Design and line fault protection scheme of a DC microgrid based on battery energy storage system. *Energies* **2018**, *11*, 1823. [CrossRef]
10. Ananda, S.A.; Gu, J.C.; Yang, M.T.; Wang, J.M.; Chen, J.D.; Chang, Y.R.; Lee, Y.D.; Chan, C.M.; Hsu, C.H. Multi-agent system fault protection with topology identification in microgrids. *Energies* **2017**, *10*, 28. [CrossRef]
11. Afamefuna, D.; Chung, I.Y.; Hur, D.; Kim, J.Y.; Cho, J.T. A techno-economic feasibility analysis on LVDC distribution system for rural electrification in South Korea. *J. Electr. Eng. Technol.* **2014**, *9*, 1501–1510. [CrossRef]
12. Haghi, E.; Raahemifar, K.; Fowler, M. Investigating the effect of renewable energy incentives and hydrogen storage on advantages of stakeholders in a microgrid. *Energy Policy* **2018**, *113*, 206–222. [CrossRef]
13. Han, S.K.; Choi, H.J.; Cho, S.H. Capacity optimizing method of distributed generators in stand-alone microgrid considering grid link-characteristics. *J. Electr. Eng. Technol.* **2018**, *13*, 1483–1493.
14. Kann, S.; Shiao, M.J.; Honeyman, C.; Perea, A.; Jones, J.; Smith, C.; Gallagher, B.; Moskowitz, S.; Baca, J.; Rumery, S.; et al. U.S. Solar Market Insight Report 2016 Q2. Available online: https://www.seia.org/research-resources/solar-market-insight-report-2016-q2 (accessed on 20 July 2018).
15. Nykvist, B.; Nilsson, M. Rapidly falling costs of battery packs for electric vehicles. *Nat. Clim. Chang.* **2015**, *5*, 329–332. [CrossRef]
16. Hanna, R.; Ghonima, M.; Kleissl, J.; Tynan, G.; Victor, D.G. Evaluating business models for microgrids: Interactions of technology and policy. *Energy Policy* **2017**, *103*, 47–61. [CrossRef]
17. Hassan, A.S.; Cipcigan, L.; Jenkins, N. Optimal battery storage operation for PV systems with tariff incentives. *Appl. Energy* **2017**, *203*, 422–441. [CrossRef]
18. Jung, J.; Villaran, M. Optimal planning and design of hybrid renewable energy systems for microgrids. *Renew. Sustain. Energy Rev.* **2017**, *75*, 180–191. [CrossRef]
19. Hanna, R.; Kleissl, J.; Nottrott, A.; Ferry, M. Energy dispatch schedule optimization for demand charge reduction using a photovoltaic-battery storage system with solar forecasting. *Sol. Energy* **2014**, *103*, 269–287. [CrossRef]
20. Nottrott, A.; Kleissl, J.; Washom, B. Energy dispatch schedule optimization and cost benefit analysis for grid-connected, photovoltaic-battery storage systems. *Renew. Energy* **2013**, *55*, 230–240. [CrossRef]
21. Pless, J.; Arent, D.J.; Logan, J.; Cochran, J.; Zinaman, O. Quantifying the value of investing in distributed natural gas and renewable electricity systems as complements: Applications of discounted cash flow and real options analysis with stochastic inputs. *Energy Policy* **2016**, *97*, 378–390. [CrossRef]
22. Husein, M.; Chung, I.Y. Optimal design and financial feasibility of a university campus microgrid considering renewable energy incentives. *Appl. Energy* **2018**, *225*, 273–289. [CrossRef]
23. Database of State Incentives for Renewables & Efficiency. Available online: http://www.dsireusa.org/ (accessed on 25 July 2018).
24. Soto, W.D.; Klein, S.A.; Beckman, W.A. Improvement and validation of a model for photovoltaic array performance. *Sol. Energy* **2006**, *80*, 78–88. [CrossRef]
25. Amrollahi, M.H.; Bathaee, S.M.T. Techno-economic optimization of hybrid photovoltaic/wind generation together with energy storage system in a stand-alone micro-grid subjected to demand response. *Appl. Energy* **2017**, *202*, 66–77. [CrossRef]
26. Manwell, J.F.; McGowan, J.G. Lead-acid battery storage model for hybrid energy sysems. *Sol. Energy* **1993**, *50*, 399–405. [CrossRef]
27. U.S. Department of Energy. *Fuel Cell Handbook*; EG&G Inc.: Morgantown, WV, USA, 2004.
28. Kaldellis, J.M. *Stand-Alone and Hybrid Wind Energy Systems*; CRC Press: Boca Raton, FL, USA, 2010.
29. Myers, B. *Principles of Corporate Finance*; McGraw-Hill: New York, NY, USA, 2003.

30. U.S. Utility Rate Database. Available online: https://openei.org/apps/USURDB/?utilRateFinder=SDG%26E&service_type=&is_default=&search=&page=1 (accessed on 13 September 2018).
31. Power Project Data Sets. Available online: https://power.larc.nasa.gov/ (accessed on 13 September 2018).
32. Renewables Portfolio Standard. Available online: http://programs.dsireusa.org/system/program/detail/840 (accessed on 25 July 2018).
33. Renewable Market Adjusting Tariff (ReMAT). Available online: http://programs.dsireusa.org/system/program/detail/5665 (accessed on 25 July 2018).
34. Business Energy Investment Tax Credit (ITC). Available online: http://programs.dsireusa.org/system/program/detail/658 (accessed on 25 July 2018).
35. Self-Generation Incentive Program. Available online: http://programs.dsireusa.org/system/program/detail/552 (accessed on 25 July 2018).
36. Net Metering. Available online: http://programs.dsireusa.org/system/program/detail/276 (accessed on 25 July 2018).
37. Modified Accelerated Cost-Recovery System (MACRS). Available online: http://programs.dsireusa.org/system/program/detail/676 (accessed on 25 July 2018).
38. Property Tax Exclusion for Solar Energy Systems. Available online: http://programs.dsireusa.org/system/program/detail/558 (accessed on 25 July 2018).
39. Heydari, A.; Askarzadeh, A. Techno-economic analysis of a PV/biomass/fuel cell energy system considering different fuel cell system initial capital costs. *Sol. Energy* **2016**, *133*, 409–420. [CrossRef]

© 2018 by the authors. Licensee MDPI, Basel, Switzerland. This article is an open access article distributed under the terms and conditions of the Creative Commons Attribution (CC BY) license (http://creativecommons.org/licenses/by/4.0/).